P1.5 NEAR-FIELD CORRECTIONS FOR METEOROLOGIAL RADARS

Stephen M. Sekelsky *

1. INTRODUCTION

Millimeter-wavelength (MMW) cloud radars operating at W-band (95 GHz) and Ka-band (35 GHz) are popular atmospheric research tools because they are compact, have low prime power requirements, and are highly sensitive to small hydrometeors. In order to maximize sensitivity, ground-based systems use large diameter high-gain antennas. However, these antennas have substantial far-field distances as large as several kilometers.

The far-field distance is defined as $r_f = 2D^2/\lambda$ where D is antenna diameter and λ is radar wavelength. The region $r \geq r_f$ is referred to as the far-field. Here, antenna gain and pattern shape are considered constant. The region $r < r_f$ is referred to as the near-field. Here, antenna gain and pattern shape vary with distance. Processing near-field radar measurements using the conventional radar equations gives erroneous results because these relationships assume far-field antenna characteristics. Correction factors are needed to account for the radar response to targets that lie in the near-field.

This abstract presents general near-field reflectivity and gain corrections that depend only on r/r_f. They are independent of other radar characteristics, including transmit pulse length, receiver bandwidth and antenna feed pattern (illumination function). Although these corrections were developed for MMW systems, they are applicable to most radars using lens or dish antennas.

2. NEAR-FIELD MODEL

Although several antenna illumination functions and edge tapers were modeled, the universal correction factors presented here assume cosine on a pedestal illumination with -12 dB edge taper. Edge tapers levels between -10 dB and -12 dB are typical for dish and lens antennas because they yields the highest overall antenna efficiency (Stutzman and Thiele 1981). Gain and other pattern characteristics are relatively insensitive to the shape of the feed illumination pattern for this span of tapers.

2.1 Radar Reflectivity Calculation

Various articles and texts describe radar scattering from hydrometeors (Battan, 1973; Smith, 1984; Sauvageot, 1992; Doviak and Zrnic', 1984). In each case, the meteorological form of the radar equation is simplified using far-field approximations for the antenna gain and antenna pattern shape such that

$$\overline{P}_r = \frac{Z_e}{R_c r_o^2 l_{atm}^2}, \qquad (1)$$

where

Z_e = equivalent radar reflectivity factor ($mm^6 m^{-3}$),

$\overline{P}_r$ = average received power referenced to digitizer input (mW),

r_o = range to center of sampling volume (km),

R_c = radar constant,

l_{atm} = one-way path integrated atmospheric loss.

Z_e denotes the possibility of Mie scattering and is appropriate for MMW systems (Ulaby et. al., 1982, Lhermitte, 1988). Following Doviak and Zrnic', (1984), R_c is determined from radar specific constants and assumes a circularly symmetric Gaussian antenna pattern.

Because R_c assumes constant far-field antenna gain and pattern shape, (1) is strictly valid only for $r_o \geq r_f$. Equation (1) can be modified to account for near-field effects by multiplying with a correction factor, $(F(r_o)/F_o)$, which accounts for the the near-field reduction in scattering from volume targets:

$$P_r = \left(\frac{Z_e}{R_c r_o^2 l_{atm}^2}\right)\left(\frac{F(r_o)}{F_o}\right). \qquad (2)$$

F is the normalized pulse radar response to volume targets and is defined as

$$F(r_o) \approx r_o^4 \int_0^{\pi}\int_0^{2\pi} S^2(r_o,\theta,\phi) sin(\theta) d\theta d\phi. \qquad (3)$$

In the far-field F is independent of range. F_o is simply this constant far-field value, F_o=$F(r_o = \infty)$.

2.2 Aperture Antenna Model

Electric (E) and magnetic (H) field intensities are calculated for an aperture using the magnetic vector potential, $\overline{A}$, (Stutzman and Thiele, 1981; Balanis, 1982). For a known source current distribution, $\overline{J}$

*Microwave Remote Sensing Lab., Univ. of Massachusetts at Amherst, Amherst, MA, email:sekelsky@mirsl.ecs.umass.edu

$$\overline{A} = \int_V \overline{J} \frac{e^{-j\beta R}}{4\pi R} dV, \quad (4)$$

where $\beta = 2\pi f\sqrt{\mu_o \epsilon_o}$, and $R = |\bar{r} - \bar{r}'|$. $\bar{r}$ is the vector from the origin to the field point and $\bar{r}'$ is the vector from the origin to an elemental source location. The source current distribution or illumination function, J, determines the shape of the antenna radiation pattern. For cosine on a pedestal illumination:

$$J(r') = C + (1 - C)cos(2\pi r/D) \quad (5)$$

where $20log(C)$ is the edge taper illumination.

Power flow in the radial direction is determined from the magnetic and electric field components parallel to the aperture plane. Antenna radiation fields are calculated using the the Poynting vector,$\bar{S}$, which represents the time-averaged real power flow.

Knowledge of either E or H is sufficient to determine $\bar{S}$ since they are related by the characteristic impedance of free space, $Z_o = E/H$. This method is also more computationally efficient. Using H, $\bar{S}$ is calculated as

$$\overline{S} = \frac{Z_o}{2} \left|\overline{H}\right|^2, [W m^{-2}]. \quad (6)$$

$Z_o = \sqrt{(}\mu_o/\epsilon_o)$, which is approximately 377 Ohms. $\mu_o = 4\pi \times 10^7$ Henry/m is the permeability of free space and $\epsilon_o = 8.854 \times 10^{-12}$ Farads/m is the permittivity of free space (Balanis 1989). H is determined from A using the following relationship:

$$\overline{H} = \frac{1}{\mu} \overline{\nabla} \times \overline{A}. \quad (7)$$

The integral in (6) is evaluated numerically and the derivative in (7) is evaluated by using finite differences. The accuracy of these numerical calculations has been verified by comparison to published and analytical results for several common aperture distributions.

3. NEAR-FIELD REFLECTIVITY CORRECTION

The universal near-field reflectivity correction given below is a fit to (8) for cosine on a pedestal illumination with -12 dB edge taper:

$$\frac{F(r_o)}{F_o} = \frac{5.26x10^{-5} + (r_o/r_f)^{2.50}}{0.0117 + (r_o/r_f)^{2.50}}. \quad (8)$$

Equation (8) is valid for $r_o \geq 0.025 r_f$, which is less than the 100 m minimum range, which is typical of pulsed MMW systems.

4. NEAR-FIELD BORESIGHT GAIN CORRECTION

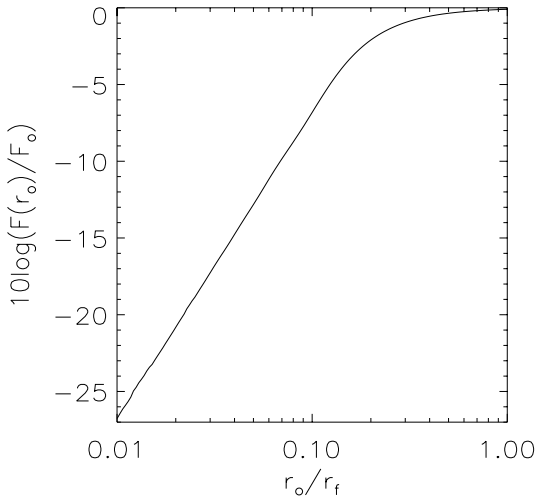

Figure 1: Near-field reflectivity reduction versus r_o/r_f.

A near field boresight gain correction is useful for measuring point targets and for external system calibrations using corner reflectors, etc. There are several reasons for performing external calibrations in the near-field. First, the calibration site may not have clear line-of-sight between the radar and calibration target if the target is located in the far-field. Second, the radar footprint size is proportional to distance so that unwanted reflections from the surface and vegetation that influence calibration measurements are minimized by calibrating at short range.

Simulations show that in the near-field, antenna boresight gain, $G(r_o)$, is reduced from its constant far-field value, G_o. Therefore, the power reflected from a calibration target measured at the radar receiver is underestimated. This leads to over-estimation of the radar constant, R_c.

The universal boresight gain correction given below is also derived from the antenna power density pattern simulations described in Section 2.1.

$$(G(r_o)/G_o) = \frac{-0.00472 + 1.0(r_o/r_f)^{2.04}}{0.00633 + (r_o/r_f)^{2.04}}. \quad (9)$$

The near-field power reduction for point targets, such as a corner reflector, is then given as

$$(G(r_o)/G_o)^2 = \frac{-0.0066 + 1.0(r_o/r_f)^{2.08}}{0.0152 + (r_o/r_f)^{2.08}}, \quad (10)$$

Unlike the reflectivity correction, $G(r_o)/G_o$ does not monotonically increase with range within the near-field. Fig-

ure 2 shows this behavior, which is similar to that predicted by Hansen (Hansen 1985). As with the reflectivity correction, the gain reduction $G(r_o)/G_o$ is also insensitive to illumination function and edge taper.

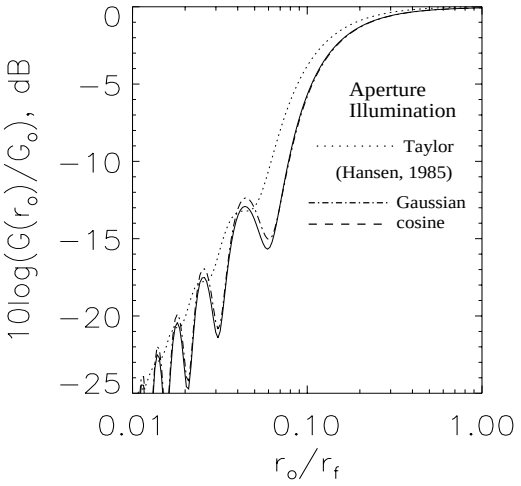

Figure 2: Boresight gain reduction for various illumination functions.

5. MEASUREMENTS

Measurements from the one-meter-diameter antenna CPRS Ka-band radar and from the three-meter-diameter antenna U.S. Department of Energy ARM millimeter-wave Cloud Radar (MMCR) system (Moran et al. 1998) are compared in order to verify the accuracy of the universal reflectivity correction given in (8). Figure 3 plots profiles of radar reflectivity versus r_o/r_f. The solid line represents the ratio of near-field corrections for MMCR and CPRS.

6. CONCLUSIONS

Antenna near-field patterns are simulated to determine near-field correction factors for use with far-field reflectivity and calibration equations. Antenna simulations presented in this paper assume a circular aperture, and an illumination pattern and edge taper that are typical of most lens and dish antennas. Radar reflectivity simulations for various illumination functions and edge tapers show that the reflectivity correction factor, $F(r_o)/F_o$, and antenna gain correction, $G(r_o)/G_o$, are not sensitive to illumination function shape, or to edge taper for edge tapers of approximately -10 dB to -12 dB, a fortunate result since most dish and lens antennas use this range of edge taper because it maximizes antenna efficiency.

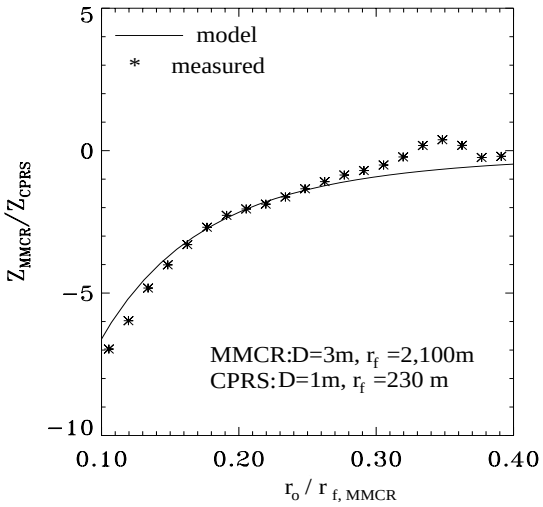

Figure 3: Ratio of Ka-band (35 GHz) reflectivity profiles measured by the UMass CPRS radar (D = 1 m) and the U.S. DOE MMCR radar (D = 3 m). For the horizontal axis, $r_{f,MMCR} = 2,100m$ is the MMCR far-field distance. The solid line is the theoretical ratio and the symbols represent measurements.

References

Balanis, C., 1982: *Antenna Theory: Analysis and Design.* Harper and Row.

Balanis, C., 1989: *Advanced Engineering Electromagnetics.* John Wiley and Sons.

Battan, L. J., 1973: *Radar Observation of the Atmosphere.* The University of Chicago Press.

Doviak, R. J. and D. S. Zrnić, 1984: *Doppler Radar and Weather Observations.* Academic Press, Inc.

Hansen, R., 1985: *Microwave Scanning Antennas.* Peninsula Publishing, Los Altos.

Lhermitte, R. M., 1988: Cloud and precipitation remote sensing at 94 GHz *IEEE Trans. Geosci. Remote Sens. 26*, 207–216.

Moran, K., B. Martner, M. Post, R. Kropfli, D. Welsch, and K. Widener, 1998: An unattended cloud-profiling radar for use in climate research *Bulletin of the American Meteorological Society 79*, 443–455.

Sauvageot, H., 1992: *Radar Meteorology.* Artech House.

Smith, P. L., 1984: Equivalent radar reflectivity factors for snow and ice particles *Journal of Climate and Applied Meteorology 23*, 1258–1260.

Stutzman, W. and G. Thiele, 1981: *Antenna Theory and Design.* Wiley.

Ulaby, F., R. Moore, and A. Fung, 1982: *Microwave Remote Sensing; Active and Passive vol. 1.* Artech House.